On-Device Reliability Assessment and Prediction of Missing Photoplethysmographic Data Using Deep Neural Networks

Monalisa Singha Roy, *Student Member, IEEE*, Biplab Roy, *Member, IEEE*, Rajarshi Gupta, *Member, IEEE*, and Kaushik Das Sharma, *Member, IEEE*

***Abstract*—Photoplethysmographic (PPG) measurements from ambulatory subjects may suffer from unreliability due to body movements and missing data segments due to loosening of sensor. This paper describes an on-device reliability assessment from PPG measurements using a stack denoising autoencoder (SDAE) and multilayer perceptron neural network (MLPNN). The missing segments were predicted by a personalized convolutional neural network (CNN) and long-short term memory (LSTM) model using a short history of the same channel data. Forty sets of volunteers' data, consisting of equal share of healthy and cardiovascular subjects were used for validation and testing. The PPG reliability assessment model (PRAM) achieved over 95% accuracy for correctly identifying acceptable PPG beats out of total 5000 using expert annotated data. Disagreement with experts' annotation was nearly 3.5%. The missing segment prediction model (MSPM) achieved a root mean square error (RMSE) of 0.22, and mean absolute error (MAE) of 0.11 for 40 missing beats prediction using only four beat history from the same channel PPG. The two models were integrated in a standalone device based on quad-core ARM Cortex-A53, 1.2 GHz, with 1 GB RAM, with 130 MB memory requirement and latency ∼0.35 s per beat prediction with a 30 s frame. The present method also provides improved performance with published works on PPG quality assessment and missing data prediction using two public datasets, CinC and MIMIC-II under PhysioNet.**

***Index Terms*—Convolutional neural network, photo plethysmogram (PPG), on-device measurement, prediction of missing data, reliability assessment, stack denoising autoencoder.**

I. Introduction

PHOTOPLETHYSMOGRAPHY (PPG) provides measurement of blood volume changes with each cardiac cycle due to the interaction of light and peripheral tissue of the skin [1]. Over the last decade, development of low power oximeters [2], [3] has been the prime impetus of wearable vital sign monitoring systems [4],[5]. Use of PPG technology has enabled surrogate measurements of many cardiovascular and hemodynamic parameters [6], [7]. Long-term recording of PPG signal is mostly carried out in intensive care units (ICU) for SpO2 and heart rate variability (HRV) analysis. Baseline modulation, a common problem in PPG measurements due to voluntary respiration, requires corrective actions for faithful diagnosis [8], [9].

Two common problems in ambulatory PPG measurements are motion artifacts (MA), and missing data segments resulting from occasional loosening of the sensor. Mitigation of these two problems can enhance the reliability in computerized decision making. Published research on PPG signal quality assessment (SQA) can be broadly classified under three categories. First, waveform morphology analysis [10], [11] or extracting time domain features being fed to different classifiers like decision tree [12], Bayesian hypothesis testing [13] and support vector machine (SVM). The second is based on signal quality index (SQI), and includes comparing the PPG pulse with previously detected pulses within a time frame [14], extracting morphological, statistical and spectral features [15] and reliable heart rate value estimated from Electrocardiogram and PPG [16], using multichannel adaptive filter (MCAF) to detect point-by-point SQI [17]. The third, machine learning based model includes dynamic time wrapping method with multilayer perceptron neural network (MLPNN) [18], statistical parameters extraction and classification and regression tree (CART) based model [19] and convolutional neural network (CNN) [20]. Published research on SQA reports only three hardware implementations, viz., time-domain features based Bayesian hypothesis testing [13], autocorrelation based method [21] and hierarchical decision rules [22]. Few limitations of the existing researches on SQA are: requirement of simultaneous measurement of other physiological signals, sensitivity of time domain features towards the MA, and inability to prescribe optimal feature set for best classifier performance. Also, the statistical morphology features (like skewness) are prone to change with the waveform morphology, age and cardiac problems, and hence, have limited robustness.

Beat-to-beat variability measurements are becoming important in various clinical applications like post cardiac arrest rehabilitation [23]–[24], atrial fibrillation (AF) assessments [25], surrogate measurements like respiration from cardiac signals

Manuscript received April 30, 2020; revised July 18, 2020 and September 3, 2020; accepted September 28, 2020. Date of publication October 7, 2020; date of current version December 30, 2020. This work was supported in part by the Departmental Research Support program from University Grants Commission, India. Reference No.029/17-18/1702 dtd: Nov 30, 2017 *(Corresponding author: Rajarshi Gupta.)*

Monalisa Singha Roy, Rajarshi Gupta, and Kaushik Das Sharma are with the Electrical Engineering Section, Department of Applied Physics, University of Calcutta, Kolkata 700009, India (e-mail: monalisa_sr03@yahoo.co, in; rgaphy@caluniv.ac.in; kdsaphy@caluniv.ac.in).

Biplab Roy is with the Electronics & Communication Engineering Department, NITMAS, West Bengal 743368, India (e-mail: biplab.roy@nitmas.edu.in).

Color versions of one or more of the figures in this article are available online at https://ieeexplore.ieee.org.

Digital Object Identifier 10.1109/TBCAS.2020.3028935

[26] and abnormality detection [27]. Instead of discarding missing data, its prediction can improve the accuracy of such variability measurements. Prediction of missing physiological data segment is a relatively limited explored area of research. For prolonged duration recording, beat-to-beat PPG morphology can be useful for HR, respiration rate and blood pressure variability assessments. On the other hand, when the recording length is less (around 1 min) with missing segments, reconstruction is necessary for clinical evaluation. The published works are mostly implemented in simulation, and restricted to small missing segment prediction, based on correlation between multiple physiological signals which are modelled by adaptive filter [28], iterative retraining and accumulated averaging of NN [29], multiple template matching [30], sample entropy and bootstrapping [31] principal component analysis (PCA) [32], and PCA in conjunction with time delay neural network (TDNN) [33]. The work [34] used immediately preceding clean PPG data from same channel for prediction of maximum 10 MA corrupted/ missing beats using recurrent neural network (RNN) with acceptable accuracy.

On-device analysis of physiological signals is becoming gradually popular [6] in the recent years due to the advent of low-power, resource-constrained embedded computing. These can save time in diagnosis, as well as provide on-site diagnosis to relieve processing burden of centralized systems. The present research work describes a deep neural network (DNN) based approach for PPG reliability assessment and prediction of missing data segments, and their on-device implementation. The main contributions of the current work are

- On-device implementation of a generic lightweight intelligent model based on a stacked denoising autoencoder (SDAE) and a MLPNN for PPG reliability assessment, to achieve a good agreement with experts' annotations.
- Real-time prediction of missing segment with good accuracy (RMSE of 0.22) using a long short term memory (LSTM) neural network combined with CNN using a short history (as short as 4 beats) of the same channel data. For prediction, both the acceptable and MA corrupted beats of PPG data history were considered that are expected to real situation.
- Preservation of other physiological information like respiration, heart rate (HR) in the predicted PPG segments, first time addressed in published research.
- Hardware implementation of the proposed reliability assessment model and missing beat prediction models in a standalone system (ARM Cortex A-53 at 1.2 GHz with 1 GB RAM).

To the best of authors' knowledge, the proposed research is the first on-device integrated approach for PPG reliability assessment with prediction of missing segments. The proposed technique was validated with volunteers' data collected at laboratory, PhysioBank MIMIC-II database and 2010 Computing in Cardiology (CinC)/PhysioNet Challenge dataset [35]. The layout of the paper is as follows: section II describes various methods constituting the working flow of the proposed research, section III and IV provides and discusses the results respectively with volunteers' data, MIMIC-II and CinC data with hardware implementation issues. Section V provides on-device implementation information and highlights few limitation of the present research. Section VI, Conclusion states the main outcome of the research.

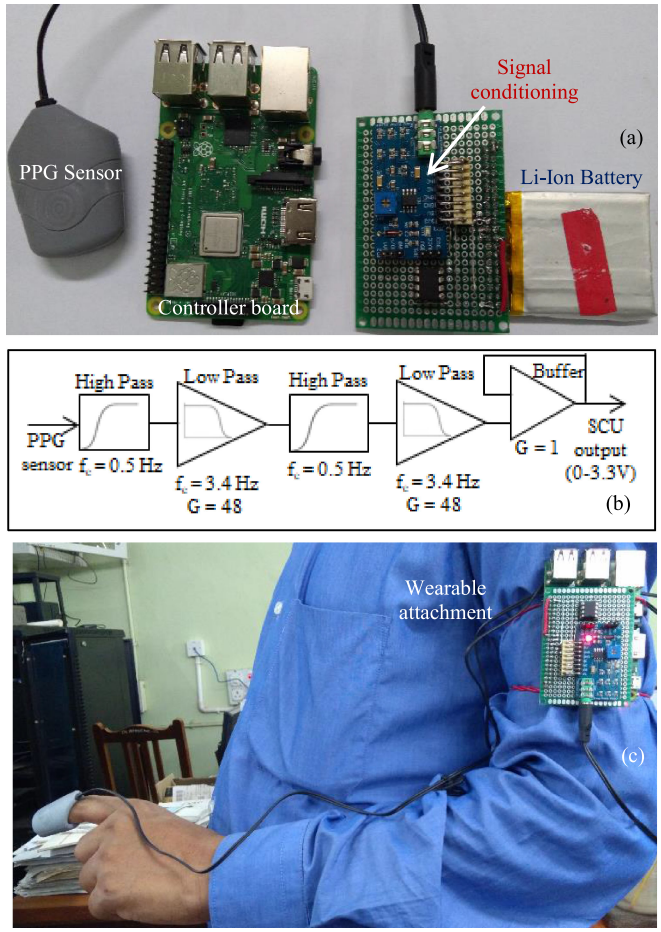

Fig. 1. (a) Components used for hardware implementation. (b) Block schematic of signal conditioning unit (f_c: cut-off frequency and G: gain). (c) Standalone wearable laboratory prototype photograph.

II. Methodology

A. Hardware Test-Bed of the Work

The hardware components used for the real-time SQA and prediction of missing segments scheme from PPG is shown in Fig. 1(a). A transmission type commercial PPG sensor is interfaced with a signal conditioning unit (SCU) [36]–[37]. The block schematic of SCU is shown in Fig. 1(b), consisting of two-stage combination of a high pass (0.5 Hz) and a low-pass filter (3.4 Hz). The SCU generates an output in the range 0-3.3 V. This is digitized at 60 Hz by a SPI type AD converter (MCP3202) and fed to a standalone computing system with a quad-core ARM Cortex-A53 controller operating at 1.2 GHz, supported by 1 GB RAM. The entire unit is powered by a Li-Ion battery. The laboratory prototype can be attached to upper part of arm to form a wearable attachment as shown in Fig. 1(c).

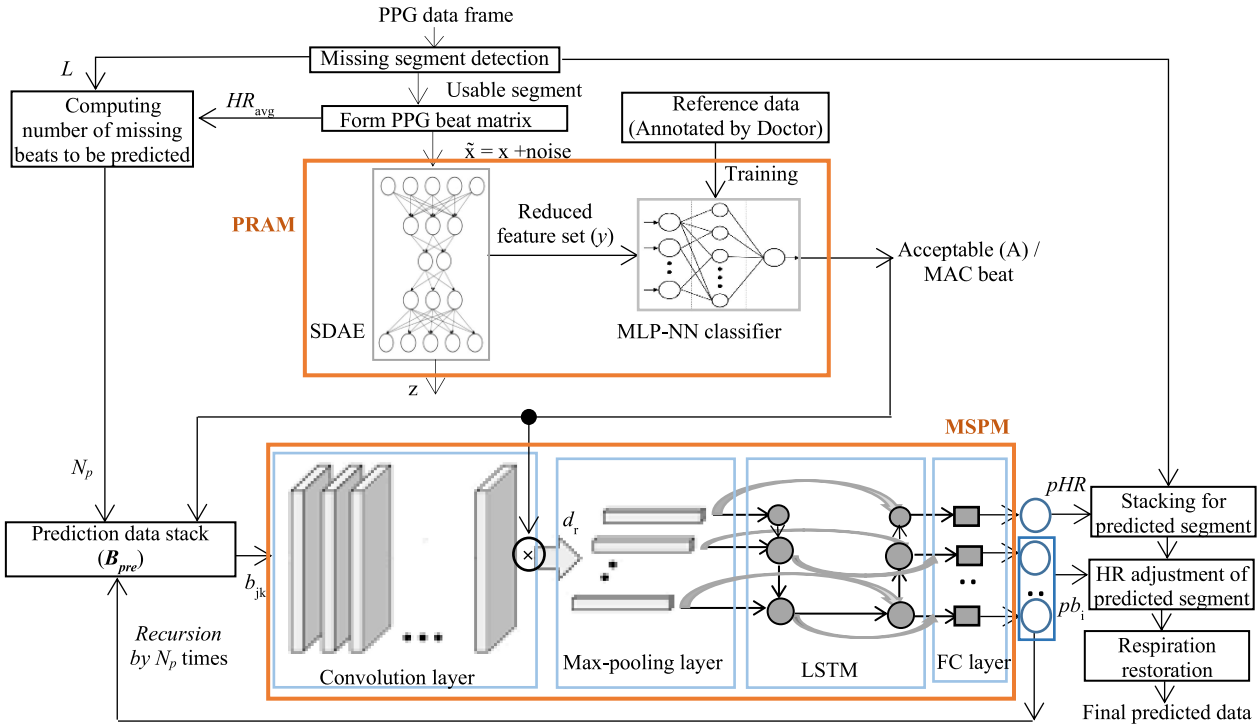

Fig. 2. Signal Processing block diagram.

B. Signal Processing Flow

The signal processing flow diagram of the entire work is shown in Fig. 2. There are main two blocks, viz., PPG reliability assessment model (PRAM) and missing segment prediction model (MSPM). At first, any missing segment representing loosening of sensor is found out in the current data frame. This is 'unusable' since since it carries no clinical information. The rest, representing either clean or MA corrupted PPG data is 'usable' segment. The PRAM evaluates this usable segment and classifies each beat (or cardiac cycle) as acceptable (good quality) or MA corrupted (bad quality) by a combination of SDAE and MLPNN. The missing segment, if any, in the data frame is predicted by utilizing a prediction data stack (PDS) a collection of short duration preceding beats, through the MSPM. The following subsections provide brief detail of the signal processing blocks.

C. Initial Preprocessing and Data Preparation

The usable segment is detected by a slope based approach. For missing segments, either a series of constant values, or, some arbitrary values with minor fluctuation is obtained. From the usable segment, a 2-D matrix is formed aligning the systolic peaks and padding both ends with last sample's values, using the technique described in [38].

The 2-D beat matrix $\boldsymbol{X}$ can be represented as:

$$X = [x_1 \ x_2 \ \ldots\ldots\ldots x_k \ ]_{M\times N} \tag{1}$$

where, N is the number of beats and M is the number of samples including padding in each beat. The average heart rate (HR_{avg}) of the frame is computed as:

$$HR_{avg} = \frac{\sum_k HR_k}{N} \tag{2}$$

$HR_k = \frac{60}{l_k \times s}$ where, l_k is the number of samples excluding the padding, HR_k is the heart rate in kth beat and s is the sampling interval in second. The samples beyond the coverage of this beat matrix, denoting the part of incomplete beats, are discarded and the missing segment length (L) was modified accordingly. The tentative number of predicted beats (N_p) is estimated as:

$$N_p = int\left(\frac{L}{HR_{avg}}\right), \ res = mod\left(\frac{L}{HR_{avg}}\right) \tag{3}$$

where, '*int*' stands for the integer division and '*mod*' stands for modular division, '*res*': number of 'excess' samples to be adjusted among predicted N_p beats according to the predicted HR.

D. PPG Reliability Assessment Model (PRAM):

The first stage of SDAE is the mapping of a single PPG beat (x) from the usable segment into $\tilde{x}$ by adding stochastic noises using corruption process $Q(x|\tilde{x})$ [39]. A DAE is intended to extract compressed representation (y) of input ($\tilde{x}$) through unsupervised modification of weights (w) and bias (b) of encoder and decoder. Mathematically, the operations can be represented as:

$$y_k = \emptyset_e \ (w_e\tilde{x}_k + b_e) \ z_k = \emptyset_d \ (w_e y_k + b_d) \tag{4}$$

where, subscript $e(d)$ stands for encoder (decoder), z is decoder output, $\Phi(\cdot)$ is the nonlinear activation function (sigmoid), and k is the instance of the beat. The DAE has 4 hidden layers

for encoder and decoder. The average ACC of the PRAM was tested with different number of features, fed to the SDAE using test dataset. From SDAE, extracted features (y) are fed to the MLPNN model, represented as:

$$z_{oj} = \emptyset\left(\sum_i y_j w_{ao} + b\right) \tag{5}$$

where, y_j is the jth input feature array, b is the bias, z_{0j} is the output and w_{ao} is the weight matrix. The classification rule is formed as: $Y \in' A'$ if $Y > D_t$

$$\in' C' \text{otherwise}$$

Where, D_t: threshold value determined by group reference volunteers data (healthy or, N and cardiovascular disease, or, CVD), in consultation with expert annotated data. The MLPNN has 4 deep layers with rmsprop optimization. Model is designed using Keras runs on top of TensorFlow. Each PPG record (one reference clean PPG and 10 partially corrupted records with various noise levels) from N and CVD group was independently annotated as 'acceptable' ('A') or 'MA corrupted' ('MAC') during training and testing of the PRAM. 10-fold cross validation was performed at the time of training the PRAM with an average MSE of 0.0006.

E. CNN-LSTM Based Missing Segment Prediction Model (MSPM)

A 1-D CNN is utilized to convert the PPG samples in PDS into multi-dimensional features through a series of convolution operations [40]. The model is designed with time step length: 4, stride: 1, kernel: 8, pool size: 2. It accepts one PPG beat from PDS and generates the predicted heart rate (*pHR*) and corresponding predicted beat (*pb*) samples in the missing segment at a time. By recursion of N_{p} times, all missing beats are generated.

If $b_g = [b_1\ ,\ b_2\ \ldots\ldots\ldots b_n\ ]$ is the g^{th} PPG beat in the PDS containing n samples, the output of the l^{th} convolutional layer is:

$$c_i^{l,r} = \sigma\left(\sum_{m=1}^{M} w_m^{l,r} b_{i+m-1}^{l-1,r} + d_r^l\right) \tag{6}$$

where, σ is the ReLU activation function, m is the index value of each kernel filter, is the weight of the feature map r and filter index m and d_r is the bias for the r^{th} feature map. The influence of the MAC beats in the prediction is minimized by a masking vector d_m before the max-pooling layer:

$$f_u = [f_{ru}]\ {}^{\circ}[d_m]^T \tag{7}$$

where, f_u is the feature vector of the unacceptable beat and $d_m = 1$ or 0 alternatively, representing masking operation and '$\circ$' represents Hadamard product. The 'max-pooling' function is applied on each feature vector to generate maximum value among set of nearby input and can be expressed by:

$$P_i^{l,r} = \max_{v \in R}\left(c_{i\times s+v}^{l,r}\right) \tag{8}$$

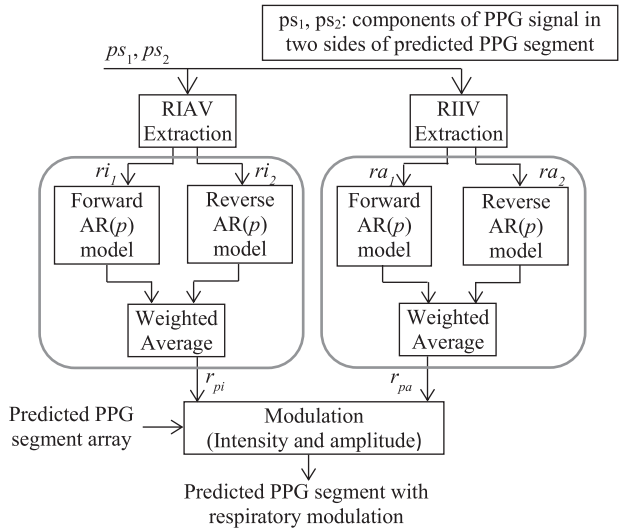

Fig. 3. Scheme of respiration information restoration in PPG data.

where, R is the input vector whose resolution is reduced by the convolution operation and s is a stride that determines how far to move along the pooled area. Here, a simple and fixed CNN-LSTM model consisting of one convolution layer, one max-pooling layer, one LSTM layer and followed by one dense layer have been used.

As shown in Fig. 2, the extracted features from the PDS along with their HR information is fed to train the LSTM layer for prediction of samples of single PPG beat and its' HR. In LSTM unit, the cell remembers the values over different time interval and three gates are used to control the flow of information contained in a cell status [39].

$$\begin{aligned} i_t &= \sigma\left(W_{pi}P_t + W_{hi}h_{t-1} + W_{qi}{}^{\circ}q_{t-1} + d_i\right) \\ f_t &= \sigma\left(W_{pf}P_t + W_{hf}h_{t-1} + W_{qf}{}^{\circ}q_{t-1} + d_f\right) \\ o_t &= \sigma\left(W_{po}P_t + W_{ho}h_{t-1} + W_{qo}{}^{\circ}q_{t-1} + d_o\right) \end{aligned} \tag{9}$$

where, the notations i_t, f_t and o_t represent forget gate, input gate and output gate, respectively. The term P_t is used as an input to the memory cell and is the output generated at time t in the previous convolution-pooling layer, and $\boldsymbol{W}$ is the weight matrix of the LSTM unit, d is the bias vector. The output of the LSTM layer is fed to the input of the FC layer. The predicted samples of single PPG beat (pb_i) with its HR (pHR_i) at the output as given by:

$$q_t = f_t\ q_{t-1} + i_t{}^{\circ}\ \sigma\left(W_{pq}P_t + W_{hq}h_{t-1} + d_q\right) \tag{10}$$

The lengths of the each predicted PPG beats (pb_i) are adjusted by a truncation or extrapolation method [41] according to respective pHR_i.

F. Restoration of Respiration Information

This process, as detailed in Fig. 3, requires usable PPG segment from both sides of the missing segment. This involves three steps, viz., (a) extraction of two kinds of respiratory modulation information, viz., respiration induced intensity variation (RIIV)

and respiration induced amplitude variation (RIAV), i.e., $ri_1(ri_2)$ and $ra_1(ra_2)$ respectively from preceding and following usable segment (reference to missing segment) using the technique as detailed in [38], (b) prediction of the RIIV (r_{fi}, r_{bi}) and RIAV components (r_{fa}, r_{ba}) using the forward and reverse auto regressive model [42]; and (c) imposing the RIIV (r_{pi}) and RIAV (r_{pa}) on the predicted PPG beats by CNN-LSTM model for respiration modulation. The respiration signal was modeled as an autoregressive (AR) process of order p[AR(p)] as:

$$y\ [n] = \sum_{k=1}^{p} a_k\ y\,[n-k] + \epsilon \tag{11}$$

where, ϵ: the prediction error; $a_{k:}$: the AR coefficients; $y[n]$: nth predicted sample of AR process. An autoregressive (AR) process can be modeled and implemented as a simple IIR filter with recursive architecture where the filter coefficients are matched such as to produce the signal it is going to fit and optimized in least square sense. The coefficients are to be chosen such that the system remain stable and so, the poles of the filter, which is an all-pole filter will have to be within the unit circle in z-domain. Here, a 2nd order AR model is implemented to compute a_k as:

$$f\ = \frac{1}{2\pi}\cos^{-1}\left[\frac{a_1\,(a_2-1)}{4a_2}\right] \tag{12}$$

The best suitable values of a_k, which gives the minimum prediction MSE (ϵ) is used. A forward and backward model using Levinson-Durbin recursion [42] are created and samples in the gap are taken as weighted average of those predicted from both sides as:

$$r_{p_k} = \frac{r_{f_k} w_{f_k} + r_{b_k} w_{b_k}}{w_{f_k} + w_{fb_k}} \tag{13}$$

where, k: *'i'* for RIIV and *'a'* for RIAV; r_{fk} (r_{bk}): sample with forward (backward) prediction; w_{fk} (w_{bk}); weight given to the forward (backward) predicted value in forming one predicted sample, r_p. Finally, these two predicted components ($r_{\rm pi}$ and $r_{\rm pa}$) were used to modulate the predicted PPG samples by MSPM in the form of intensity (addition) and amplitude generated modulation (multiplication) to restore the respiration information.

The A/MAC and predicted beats are tagged with A, MAC and REC respectively along with the date and time stamping in a separate data file, the raw samples are being stored in the device memory so that the unacceptable beats can be taken care of while making clinical decision from the data.

III. Experimental Results

A. Data Collection for Validation and Testing

Total 40 (N: 20 and CVD: 20) volunteers, in the age span of 23-85 years were recruited for this study with informed consent. Minimum three sets of PPG data (10 min/record) was collected from left hand index finger from each subject under sitting condition with intermittent finger movements in short duration (to simulate ambulatory scenario) using Biopac MP45 system with BSL software [43]. This constitutes the reference dataset. The test dataset was generated from reference data segments by replacing few clean parts with constant/low amplitude fluctuations to simulate sensor detachment. The clean and MA corrupted segments of the test dataset were utilized for evaluation of PRAM. The clean segments with few parts removed were utilized for evaluation of MSPM. However, the MSPM was utilized to predict only clean segments, as MA corrupted data have no clinical usage. The PRAM was also evaluated with MIMIC-II dataset under Physio Net. The MSPM was additionally tested with 2010 CinC dataset (Set A) consisting of different physiological signal (ECG, PPG, respiration etc.) In our work, only the PPG data record was used. In the initial stage of testing, the prerecorded data (volunteers' or CinC) was read from the SD card attached to the computing hardware. For real-time operation to evaluate latency, memory engagement etc., the hardware test-bed as described in Fig. 1(c) was used.

TABLE I
Results of Pram With Training and Testing Data

Training Data		Test Data	
Beats Used	ACC	Beats Used	ACC
65000 (with 10 fold cross validation)	99.06	5000 (including doctor's annotated beat)	95.75

TABLE II
Confusion Matrix of Volunteers' Data

	Actual values (T)	Actual values (F)
Predicted values (P)	TP = 1804	FP = 226
Predicted values (N)	TN = 2956	FN = 14

B. PRAM Performance Evaluation

The PRAM performance was evaluated by computing sensitivity (SE), specificity (SP) and accuracy (ACC) for detection of acceptable PPG segments considering the expert annotated data as ground truth. Table I shows the results with training (cross-validation) and blind test data separately. An average ACC of 97.75% was obtained. The overall confusion matrix of TP, TN, FP, and FN of all volunteers' data is presented in Table II. Average ACC and F1 score of 97.66 (93.85) and 95.91(91.47) were obtained for N (CVD) group respectively. The ACC of the PRAM is evaluated as percentage of disagreement (PD) with experts' opinion, defined as:

$$PD\ = \left|\frac{C_a - C_d}{C_t}\right| \times 100 \tag{14}$$

where, c_a (c_d) are the number of acceptable PPG beats determined by PRAM (annotated by doctors) and c_t is total number of beats in the record. PRAM achieved 100% agreement with the doctor's annotation for 33% of total records. The overall PD for N and CVD group are 3.24% and 3.94% respectively using randomly selected subset of test data, using 1200 annotated PPG beats. The PRAM was validated with manually annotated PPG segment with 97.76% accuracy in real time application.

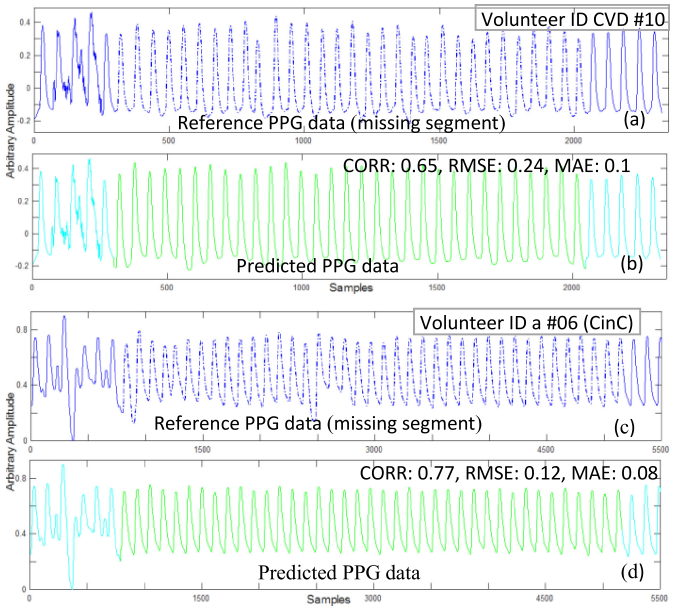

Fig. 4. MSPM performance: (a) and (c) Reference PPG from volunteer and CinC data, (b) and (d) Predicted segments from volunteer and CinC.

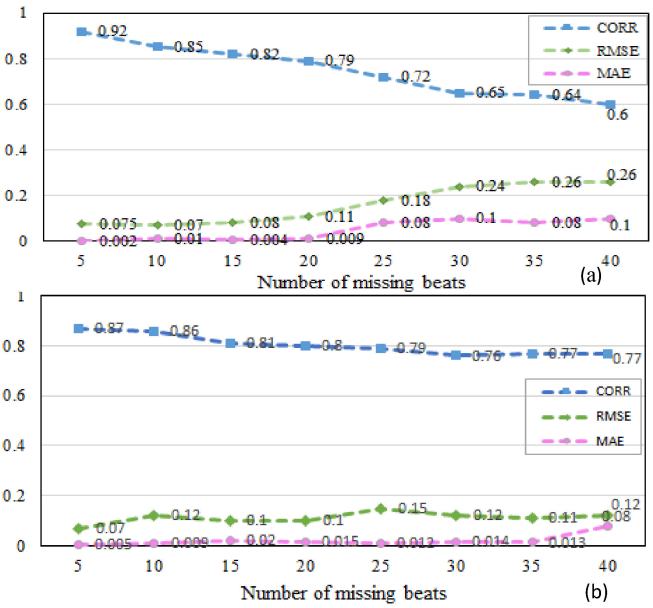

Fig. 5. Variation of CORR, MSE, and MAE with number of predicted beats: (a) With volunteer data CVD10 and (b) CinC data ID a#06.

TABLE III
MSPM PERFORMANCE WITH TRAINING AND TEST DATA

Training Data		Test Data	
Beats Used	RMSE	Beats Used	RMSE
500 (with 10 fold cross validation and time step : 4)	0.16 (best)	40 (missing beats)	0.18 (best)
	0.38 (worst)		0.43(worst)

C. MSPM Performance Evaluation

The prediction performance of MSPM was evaluated by computing the correlation coefficient (CORR), root mean square error (RMSE) and mean absolute error (MAE) between the reference and predicted PPG samples. Fig. 4 shows qualitative performance of the MSPM with reference data, considered as missing (dotted blue line-top panel) and predicted data (green line segment –lower panel) for one volunteer data (a) and (b), and one CinC data (c) and (d). The PDS, containing MAC beats is shown in cyan colour in (b) and (d). The CORR, RMSE and MAE values for the segment are also stated. Fig. 5 shows the quantitative performance of MSPM with variations of MSE, CORR and MAE for different numbers (5-40) of predicted PPG beats for same volunteer data (panel a), and CinC data (panel b) using 4 PPG beats in the PDS. As the number of missing beats increases, the CORR value gradually decreases, and RMSE and MAE value increase. These errors are mainly contributed due to the error in prediction of heart rate and respiration information.

For N (CVD) group, the average value of CORR, RMSE, and MAE are 0.73 (0.70), 0.20 (0.24) and 0.10 (0.11) respectively. Table III shows the extreme (best and worst) performance results of MSPM with a single volunteer data with training (cross-validation) and test separately.

The choice of 4 beats as PDS memory provided acceptable results considering latency and memory allocation. Each PPG record, after prediction of missing segments were independently validated by two medical experts.

The comparative performance of the PRAM with published works on SQA using manually annotated MIMIC-II data is shown in Table V. The published works on on-device SQA are mainly based on non-segmenting approach. In [13], the PPG data was tagged as 'clean' or 'corrupted' depending on baseline variation, rising count, falling count.

On device PPG quality assessment based on Arduino Due was implemented in [11], [21] and [22] using PhysioNet MIMIC-II database. In [11], PPG beat delineation and feature extraction process was implemented with 97.49% accuracy. In [21], which adopts a beat non-segmenting approach, the accuracy is higher since the contribution of a single beat on overall accuracy may be low, reducing the FP and FN cases. The quality assessment model in [22] achieved 93.21% accuracy. In [16] PPG classification model with 85.34% accuracy was achieved. The proposed work achieved competitive results with published research on SQA.

The comparative performance of MSPM with published works is shown in Table VI. In the reported works [28], [29] and [33], artificial intelligence (AI) based technique was used for missing segment prediction only from Set A record of 2010 CinC database. The performance parameters, Q_1 and Q_2 are given as [33]:

$$Q_1 = 1 - \frac{MSE}{VAR}$$
$$Q_2 = CORR \tag{15}$$

where, MSE: the mean squared error, VAR: the variance of the reference data, and CORR: the correlation coefficient between the reference and the predicted segment. In [28], filter coefficients, optimized by a PSO technique is used to reconstruct the missing segments. Since multiple physiological signals are used, they contribute more correlated features which strengthen

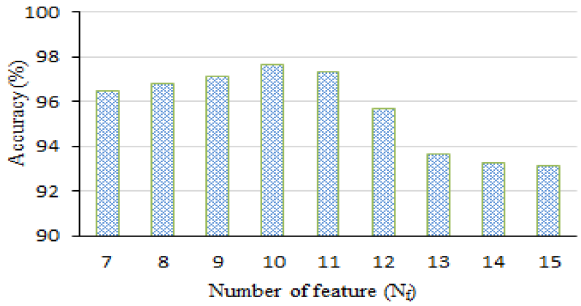

Fig. 6. PRAM performance with different features tapped from SDAE.

TABLE IV
PRAM PERFORMANCE COMPARISON WITH OTHER CLASSIFIERS

Methods	SE	SP	ACC
SVM (Kernel: sigmoid)	85.70	81.45	83.23
k-NN	89.05	84.70	87.36
Random Forest	94.47	89.21	92.90
Proposed SDAE-MLPNN	99.12	93.50	95.75

TABLE V
COMPARISON WITH EXISTING ON DEVICE SQA WORKS

Works	Method	SE (%)	SP (%)	ACC (%)
Vadrevu [11]	Waveform delineation and parameter extraction	95.63	98.86	97.49
Orphanidou [16]	Signal quality index	89.10	75.71	85.34
Vadrevu [21]	Hierarchical decision rule	99.29	95.31	97.76
Reddy [22]	First order predictor coefficient	98.22	90.71	93.21
Proposed	SDAE-MLPNN	98.65	91.43	96.55

the prediction accuracy, than features contributed by a single physiological channel. The work in [33] achieved better results in terms of Q1 and Q2, but, it used larger data volume for training. Using short history (only 4 beats) from same channel data, the proposed MSPM method achieved comparable results with published research. Secondly, in [29]–[33] multiple other physiologic signals were utilized for prediction. In [34], the missing segment of PPG data were predicted using same channel history, but could predict up to 10 beats with satisfactory results. None of the published works have achieved restoration of respiration information in the predicted PPG. The present method accomplishes this with a very low error (RMSE of 0.32).

IV. DISCUSSIONS

The best performance of PRAM was achieved with 10 number of extracted features from the DAE. Fig. 6. Shows the ACC with different number of features tapped from SDAE. The detection of acceptable PPG segments was additionally tested with other popular classifiers like support vector machine (SVM), *k*-nearest neighbour (*k*-NN) and random forest search. Table IV shows the comparative performance of the proposed method with other popular classifiers using arbitrarily selected10 volunteers from N

TABLE VI
COMPARISON WITH EXISTING PREDICTION WORKS

Works	Method	Training data length (min)	Q1	Q2
Hartman [28]	IIR filter coefficient with PSO	-	57.6	82.9
McBride [29]	Iterative retraining	5	63.7	77.5
	Accumulated Averaging	5	66.6	79.4
Sullivan [33]	TDNN	9.5	80.2*	89.1*
Proposed	CNN-LSTM	5	70.4	81.1

∗Results of single PPG record is not available. An average results for prediction of six different physiological signals are shown.

and CVD group. It clearly shows superiority of the PRAM over other classifiers. As per our knowledge and belief, no public database on PPG with annotated good (acceptable) and bad (MAC/unacceptable) quality PPG pulses is currently available. That is why, most of the reported works on PPG SQA used own human volunteers' data.

V. ON-DEVICE IMPLEMENTATION

Initially, the PyCharm IDE was used to develop the models in Python which was connected to the Raspberry-Pi's Python interpreter. The Python interpreter was used to execute standalone scripts in command line. The R-Pi was configured with all the required python libraries like TensorFlow, Keras etc. After the configuration, the PRAM and MSPM model were tested in Raspberry-pi in standalone mode. For a 30 second PPG input frame, the execution time of PRAM model is 9.05 s to identify the A/MAC beats, with a memory engagement of 128.80 MB. The execution time of MSPM model for 30 nos. of missing beat prediction was 12.75 s and memory utilization was 130.20 MB excluding OS. The screenshots of on-device implementation in a PC monitor are shown in Fig. 7 using volunteer's data (CVD-10). Panel (a) shows the tagging (A, MAC and predicted/ REC) of the PPG beats in a separate data file while they are being stored into the SD card memory. This is extremely important to assess how much of the total data collected was predicted using the MSPM model and also, how much is MAC. This would help in the clinical decision making. Panel (b) shows the overall SE, ACC and SP values using the PRAM. Panel (c) and (d) show the MSPM performance results with same dataset, predicting 30 missing PPG beats. Panel (d) shows the graphical user interface screenshot using volunteer's data. However, the use of PC monitor is not mandatory for real-time operation. The power consumption of the standalone application is 1.90 mW, as measured by a USB type power meter (model: KWS-10VA). In the proposed algorithm, the input is just a PPG data array, and deep network architecture and hyper-parameters are fixed. The complexity of both the PRAM and MSPM model are O(n) for training phase where, the n denotes the length of the training data. For testing phase, the complexity is fixed, and O(1).

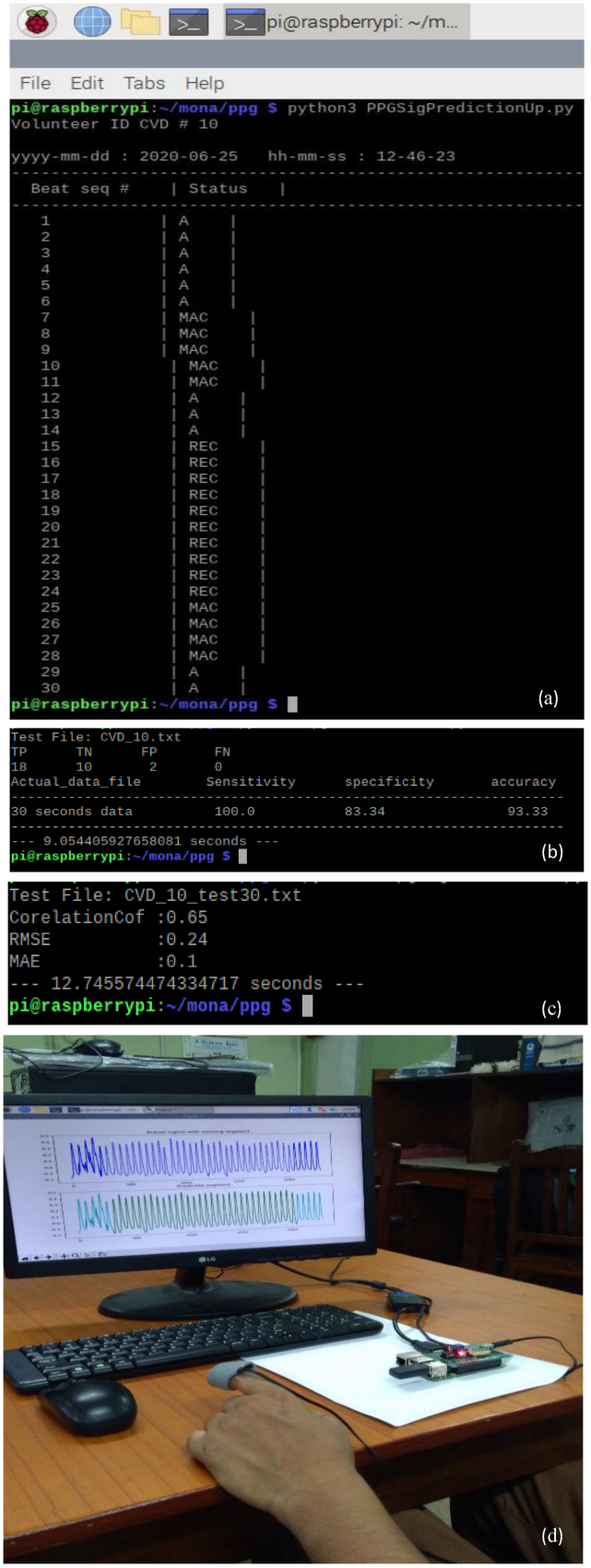

Fig. 7. Standalone implementation screenshots using CVD10 data: (a) tagging A/ MAC/REC beats for storage; (b) performance of PRAM, (c) performance of MSPM, and (d) screenshot of reconstruction.

There are the few limitations of the present research work. First, the PDS history of 4 beats must contain 2 acceptable beats to perform in a satisfactory manner. Otherwise, the PDS length is stretched to contain latest 12 PPG beats till 2 acceptable PPG beats are obtained. At the startup of predicting the missing PPG segment, a 10 s data frame with at least 4 usable (either good quality or MA corrupt) beats are required to extract the respiration information and predict the HR. Thus, in case of long chain (more than 12) of consecutive PPG beats are with MAC status / missing, the PRAM model halts and waits for at least 2 acceptable PPG beats in a pack of latest 12 beats. In such scenario, the overall latency is also increased. Secondly, in order to have respiration information restored, a short segment after the missing segment is also necessary. Thus, an input frame, typically of 40 second may have 10 usable beats (A/MAC status), 20 missing beats and 10 usable beats (A/MAC status) to have respiration information restored in the missing PPG.

VI. Conclusion

This paper presents an on-device implementation of SQA and prediction of missing segments from PPG record using a short history of same channel data using DNN-based approach. The technique was tested with 5,000 PPG beats collected from healthy (N) as well as CVD group volunteers as well as records from 2010 CinC dataset and PhysioNet MIMIC-II dataset. The proposed PRAM model could successfully identify the usable segments, close to the agreement of two medical experts with a PD of 3.5%. The MSPM model could accurately predict the missing segment (40 beats), with low reconstruction error, RMSE and MAE of 0.20 and 0.10 for N and 0.24 and 0.11 for CVD group respectively. A unique contribution was restoration of respiration modulation and HR in the predicted PPG data segment with low error (0.065 RMSE). Using only 4 beat PPG history, maximum 55 number of PPG beats could be achieved for few data with acceptable accuracy (RMSE of 0.43). The technique can be useful for long-term PPG recording.

Acknowledgement

Monalisa Singha Roy would like to thank Woman Scientist Scheme (WOS-A), Department of Science and Technology (DST), New Delhi, India. The authors extend their gratitude to Mr. Soumyak Chandra, Senior Research Assistant, for the technical support for hardware testing and troubleshooting. The authors also sincerely thank Dr. Jayanta Saha and Dr. Arunansu Talukdar, Medical College & Hospital, Kolkata and their medical expert team for clinical annotations of the PPG data records used in the study.

References

[1] J. Allen, "Photoplethysmography and its application in clinical physiological measurement," *Physiol. Meas.*, vol. 28, no. 3, pp. 1–39, 2007.

[2] K. Watanabe, S. Izumi, K. Sasai, Y. Yano, H. Kawaguchi, and M. Yoshimoto, "Low-power photoplethysmography sensor using current integration circuit for heartbeat interval acquisition," *IEEE Trans. Biomed. Circuits Syst.*, vol. 13, no. 6, pp. 1552–1562, Dec. 2019.

[3] K. N. Glaros and E. M. Drakakis, "A Sub-mW fully-integrated pulse oximeter front-end," *IEEE Trans. Biomed. Circuits Syst.*, vol. 7, no. 3, pp. 363–375, Jun. 2013.
[4] S. Song *et al.*, "A 769 μW battery-powered single-chip SoC with BLE for multi-modal vital sign monitoring health patches," *IEEE Trans. Biomed. Circuits Syst.*, vol. 6, no. 13, pp. 1506–1517, Dec. 2019.
[5] R. G. Haahr *et al.*, "An electronic patch for wearable health monitoring by reflectance pulse oximetry," *IEEE Trans. Biomed. Circuits Syst.*, vol. 6, no. 1, pp. 45–53, Feb. 2012.
[6] A. Sološenko, A. Petrenas, and V. Marozas, "Photoplethysmography-based method for automatic detection of premature ventricular contractions," *IEEE Trans. Biomed. Circuits Syst.*, vol. 9, no. 5, pp. 662–669, Oct. 2015.
[7] S. Yoshimoto, S. Hinatsu, Y. Kuroda, and O. Oshiro, "Hemodynamic sensing of 3-D fingertip force by using nonpulsatile and pulsatile signals in the proximal part," *IEEE Trans. Biomed. Circuits Syst.*, vol. 12, no. 5, pp. 1155–1164, Oct. 2018.
[8] A. A. K. Timimi, M. A. M. Ali, and K. Chellappan, "A novel AMARS technique for baseline wander removal applied to photoplethysmogram," *IEEE Trans. Biomed. Circuits Syst.*, vol. 11, no. 3, pp. 627–639, Jun. 2017.
[9] K. Li and S. Warren, "A wireless reflectance pulse oximeter with digital baseline control for unfiltered photoplethysmograms," *IEEE Trans. Biomed. Circuits Syst.*, vol. 6, no. 3, pp. 269–278, Jun. 2012.
[10] J. Abd Sukor, M. S. Mohktar, S. J. Redmond, and N. H. Lovell, "Signal quality measures on pulse oximetry and blood pressure signals acquired from self-measurement in a home environment," *IEEE J. Biomed. Heal. Informat.*, vol. 19, no. 1, pp. 102–108, Jan. 2015.
[11] S. Vadrevu and M. S. Manikandan, "Real-Time quality-Aware ppg waveform delineation and parameter extraction for effective unsupervised and iot health monitoring systems," *IEEE Sens. J.*, vol. 19, no. 17, pp. 7613–7623, Sep. 2019.
[12] J. A. Sukor, S. J. Redmond, and N. H. Lovell, "Signal quality measures for pulse oximetry through waveform morphology analysis," *Physiol. Meas.*, vol. 32, no. 3, pp. 369–384, 2011.
[13] K. Li, S. Warren, and B. Natarajan, "Onboard tagging for real-time quality assessment of photoplethysmograms acquired by a wireless reflectance pulse oximeter," *IEEE Trans. Biomed. Circuits Syst.*, vol. 6, no. 1, pp. 54–63, Feb. 2012.
[14] W. Karlen, K. Kobayashi, J. M. Ansermino, and G. A. Dumont, "Photoplethysmogram signal quality estimation using repeated Gaussian filters and cross-correlation," *Physiol. Meas.*, vol. 33, no. 10, pp. 1617–1629, 2012.
[15] M. Elgendi, "Optimal Signal Quality Index for Photoplethysmogram Signals," *Bioeng*, vol. 3, no. 4, 2016.
[16] C. Orphanidou, T. Bonnici, P. Charlton, D. Clifton, D. Vallance, and L. Tarassenko, "Signal-quality indices for the electrocardiogram and photoplethysmogram: Derivation and applications to wireless monitoring," *IEEE J. Biomed. Heal. Informat.*, vol. 19, no. 3, pp. 832–838, May 2015.
[17] I. Silva, J. Lee, and R. G. Mark, "Signal quality estimation with multichannel adaptive filtering in intensive care settings," *IEEE Trans. Biomed. Eng.*, vol. 59, no. 9, pp. 2476–2485, Sep. 2012.
[18] Q. Li and G. D. Clifford, "Dynamic time warping and machine learning for signal quality assessment of pulsatile signals," *Physiol. Meas.*, vol. 33, no. 9, pp. 1491–1501, 2012.
[19] J. D. Wander and D. Morris, "A combined segmenting and non-segmenting approach to signal quality estimation for ambulatory photoplethysmography," *Physiol. Meas.*, vol. 35, no. 12, pp. 2543–2561, 2014.
[20] T. Pereira *et al.*, "Deep learning approaches for plethysmography signal quality assessment in the presence of atrial fibrillation," *Physiol. Meas.*, vol. 40, no. 12, 2019.
[21] S. Vadrevu and M. Sabarimalai Manikandan, "Real-time PPG signal quality assessment system for improving battery life and false alarms," *IEEE Trans. Circuits Syst. II Express Briefs*, vol. 66, no. 11, pp. 1910–1914, Nov. 2019.
[22] G. N. K. Reddy, M. S. Manikandan, and N. V. L. N. Murty, "On-device integrated ppg quality assessment and sensor disconnection/saturation detection system for IoT health monitoring," *IEEE Trans. Instrum. Meas.*, vol. 69, no. 9, pp. 6351–6361, Sep. 2020.
[23] A. J. S. Webb and P. M. Rothwell, "Physiological correlates of beat-to-beat, ambulatory, and day-to-day home blood pressure variability after transient ischemic attack or minor stroke," *Stroke*, vol. 45, no. 2, pp. 533–538, 2014.
[24] G. Tian, L. Xiong, H. Leung, Y. Soo, T. Leung, and L. K. sing Wong, "Beat-to-beat blood pressure variability and heart rate variability in relation to autonomic dysregulation in patients with acute mild-moderate ischemic stroke," *J. Clin. Neurosci.*, vol. 64, pp. 187–193, 2019.
[25] J. Olbers, A. Gille, P. Ljungman, M. Rosenqvist, J. Östergren, and N. Witt, "High beat-to-beat blood pressure variability in atrial fibrillation compared to sinus rhythm," *Blood Press.*, vol. 27, no. 5, pp. 249–255, 2018.
[26] P. Langley, E. J. Bowers, and A. Murray, "Principal component analysis as a tool for analyzing beat-to-beat changes in ECG features: Application to ECG-derived respiration," *IEEE Trans. Biomed. Eng.*, vol. 57, no. 4, pp. 821–829, Apr. 2010.
[27] A. Chakraborty, D. Sadhukhan, S. Pal, and M. Mitra, "Automated myocardial infarction identification based on interbeat variability analysis of the photoplethysmographic data," *Biomed. Signal Process. Control*, vol. 57, 2020.
[28] A. Hartmann, J. M. Lemos, R. S. Costa, and S. Vinga, "Identifying IIR filter coefficients using particle swarm optimization with application to reconstruction of missing cardiovascular signals," *Eng. Appl. Artif. Intell.*, vol. 34, pp. 193–198, 2014.
[29] J. McBride, A. Sullivan, H. Xia, A. Petrie, and X. Zhao, "Reconstruction of physiological signals using iterative retraining and accumulated averaging of neural network models," *Physiol. Meas.*, vol. 32, no. 6, pp. 661–675, 2011.
[30] G. Ganeshapillai and J. Guttag, "Real time reconstruction of quasiperiodic multi parameter physiological signals," *EURASIP J. Adv. Signal Process.*, vol. 2012, no. 1, 2012.
[31] X. Dong *et al.*, "An improved method of handling missing values in the analysis of sample entropy for continuous monitoring of physiological signals," *Entropy*, vol. 21, no. 3, 2019.
[32] R. Petrolis, R. Simoliuniene, and A. Krisciukaitis, "Principal component analysis based method for reconstruction of fragments of corrupted or lost signal in multilead data reflecting electrical heart activity and hemodynamics," in *Proc. Comput. Cardiol.*, 2010, vol. 37, pp. 437–439.
[33] A. M. Sullivan, H. Xia, J. C. McBride, and X. Zhao, "Reconstruction of missing physiological signals using artificial neural networks," in *Proc. Comput. Cardiol.*, 2010, vol. 37, pp. 317–320.
[34] M. Singha Roy, P. Bag, and R. Gupta, "Reconstruction of corrupted and missing segments from photoplethysmographicdata using recurrent neural network," in *Proc. IEEE TENSYMP*, 2019, pp. 236–241.
[35] "Mind the Gap - The PhysioNet Computing in Cardiology Challenge 2010," 2010. [Online]. Available: https://physionet.org/content/challenge-2010/1.0.0/
[36] "Easy Pulse PPG sensor," [Online]. Available: http://embedded-lab.com/blog/easy-pulse-version-1-1-sensor-overview-part-1/
[37] M. Singha Roy, R. Gupta, J. K. Chandra, K. Das Sharma, and A. Talukdar, "Improving photoplethysmographic measurements under motion artifacts using artificial neural network for personal healthcare," *IEEE Trans. Instrum. Meas.*, vol. 67, no. 12, pp. 2820–2829, Dec. 2018.
[38] B. Roy and R. Gupta, "MoDTRAP: Improved heart rate tracking and preprocessing of motion-corrupted photoplethysmographic data for personalized healthcare," *Biomed. Sig. Proc. Contr.*, vol. 56, 2020.
[39] B. Du, W. Xiong, J. Wu, L. Zhang, L. Zhang, and D. Tao, "Stacked Convolutional Denoising Auto-Encoders for Feature Representation," *IEEE Trans. Cybern.*, vol. 47, no. 4, pp. 1017–1027, Apr. 2017.
[40] C. J. Huang and P. H. Kuo, "A Deep CNN-LSTM model for particulate matter (Pm2.5) forecasting in smart cities," *Sensors (Switzerland)*, vol. 18, no. 7, 2018.
[41] J. Weng, Z. Ye, and J. Weng, "An improved pre-processing approach for photoplethysmographic signal," in *Proc. IEEE Eng. Med. Biol. 27th Annu. Conf.*, 2005, pp. 41–44.
[42] Orfanidis and S. J. *Optimum Signal Processing: An Introduction*, 2nd ed. New York, NY, USA: Macmillan Pub Co, 1988.
[43] "Biopac Systems USA," [Online]. Available: https://www.biopac.com/

Monalisa Singha Roy (Student Member, IEEE) is currently working towards the Ph.D. degree in electrical engineering and applied physics from the University of Calcutta, Kolkata, India. She is currently working as a Woman Scientist Fellow (WOS-A) with the Department of Science and Technology, New Delhi, India. She has four publications in international journal and conferences. Her current research interest includes cardiovascular signal processing, artificial intelligence and system design.

Biplab Roy (Member, IEEE) is currently working as an Associate Professor with the Electronics and Communication Engineering Department, NITMAS, Kolkata, India. He has four publications in international journal and conferences. His current research interest includes cardiovascular and respiratory signal processing.

Rajarshi Gupta (Senior Member, IEEE) is currently Professor with Electrical Engineering Section, Department of Applied Physics, University of Calcutta, Kolkata, India. His research interests include biomedical signal analysis and intelligent health monitoring.

Kaushik Das Sharma (Senior Member, IEEE), is currently as a Professor with the Electrical Engineering Section of Department of Applied Physics, University of Calcutta, Kolkata, India. His research interests include fuzzy control, stochastic optimization, machine learning, robotics and systems biology.